

# On the Feasibility of Detecting Flaws in Artificial Heart Valves

Eugène S. A. M. Lepelaars, *Member, IEEE*, Willem D. R. van Ooijen, and Anton G. Tijhuis, *Member, IEEE*

**Abstract**—In this paper, we investigate the feasibility of detecting defects in certain artificial heart valves by determining the electromagnetic behavior of some simple models with the aid of thin-wire integral equations. The idea is to use the stationary current that occurs at late times after the excitation of a closed loop as a discriminator. This current exhibits an exponential decay when a resistive load is included that is representative of fatigue or a partial fracture. The decay rate is indicative of the severity of the defect. For a wire with an opening, which is representative of a complete fracture, the late-time current is completely absent. As a simplified model of remote detection by a small loop antenna that could be introduced via a catheter, we consider the coupling between two parallel circular wires. In all cases, the dispersive environment of the valve is taken to be homogeneous and filled with blood since this medium exhibits a representative dispersion.

**Index Terms**—Heart valves, integral equations, loop antennas, nondestructive testing, transient electromagnetics.

## I. INTRODUCTION

IN RECENT years, it has been established that the minor outlet closure strut in certain artificial heart valves may suffer from mechanical defects. These defects appear as cracks or fractures near the junction of a leg of this strut with the main ring of the device. As a consequence, the valve occluder may escape from the device, which subjects the patient to a lethal risk. In The Netherlands, from 1979 to 1986, the heart valve of 2303 patients was replaced by this type of artificial heart valve. At present, approximately 1500 of these patients are still alive. In the U.S., between 30 000 and 40 000 patients use such a device. An epidemiological study in 1992 [1] found 42 strut fractures during mean follow-up of 6.6 years, while a nondestructive evaluation of 24 representative explanted valves [2] showed single-leg fractures in seven and fatigue changes in two of them. Fig. 1 shows a typical valve. Fig. 2 shows an image of applying scanning electron microscopy (SEM) to a fractured leg.

In view of this development, several research groups were approached with the question whether, from their expertise, it would be possible to develop techniques for assessing the quality of existing heart valves implanted in patients. This paper presents the first steps toward using pulsed electromagnetic

Manuscript received November 24, 1999; revised May 3, 2000. This work was supported by the Netherlands Heart Foundation under Research Grant 44 064.

E. S. A. M. Lepelaars is with the TNO Physics and Electronics Laboratory, 2509 JG, The Hague, The Netherlands.

W. D. R. van Ooijen is with Arithmos Management Consultants B.V., 2518 JA, The Hague, The Netherlands.

A. G. Tijhuis is with the Faculty of Electrical Engineering, Eindhoven University of Technology, 5600 MB Eindhoven, The Netherlands.

Publisher Item Identifier S 0018-9480(00)09712-X.

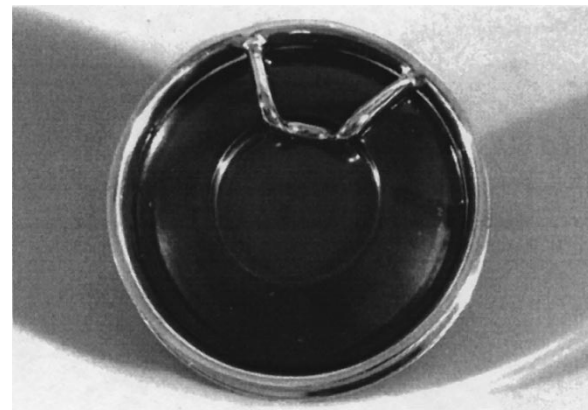


Fig. 1. Typical heart valve, where the occluder and minor strut are clearly visible.

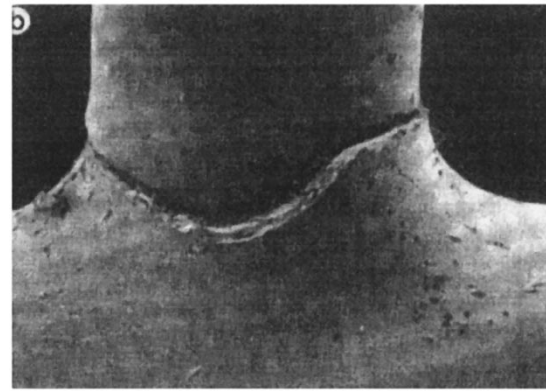


Fig. 2. SEM image of a typical heart valve with a fractured leg.

waves for this purpose. The principal difficulty with generating electromagnetic effects in a biological environment is that blood and live tissue are highly dispersive and, therefore, extremely lossy. This means that any measurement will definitely have to be invasive, e.g., via a catheter. Even in such circumstances, it seemed doubtful whether a significant electromagnetic effect can be generated and measured. To investigate this, it was decided to first model a simplified, but representative, configuration with the aid of computational techniques.

In our opinion, the model should have at least the following characteristic features of an artificial heart valve:

- 1) loop of highly conducting material representing the metal parts;
- 2) choice between closing the loop completely (perfect valve), including a resistive load (fatigue, partial fracture) or an interruption (complete fracture);

### 3) environment with representative material properties.

A simple model satisfying these conditions is a circular wire embedded in a homogeneous dielectric medium. An electric current along the wire is excited by a delta-gap voltage pulse  $V(t)$  or by an incident field  $\mathcal{E}^i(\mathbf{r}, t)$ , both of finite duration. The wire is assumed to be thin enough that the thin-wire approximation may be applied. We consider voltage excitation directly on the wire, and remote excitation by a pulsed magnetic point dipole. Both these sources induce an almost stationary current at late times, with a decay rate that is indicative of the quality of the loop.

The model of a single loop is a considerable simplification of the actual situation. In particular, the problem of detecting the late-time behavior of the current is not addressed. A logical next step is to replace the magnetic dipole, which may be envisaged as a small current loop with an externally impressed current, by a larger loop excited by a delta-gap voltage source, and to study the current in both loops. The secondary loop is excited by a Gaussian voltage pulse. Since this loop is assumed to be perfect, a step-like current is generated, which causes an electric field resembling the dipole field used above. The results indicate that it indeed may be possible to use a secondary loop for the remote induction and detection of the desired current.

The paper is organized as follows. In Section II, we describe the three single-wire models and specify the relevant integral equations. The numerical solution of these equations and the results obtained are discussed in Section III. The principle of detection by a second loop is addressed in Section IV. Finally, the most important conclusions are stated in Section V.

## II. SINGLE-WIRE MODELS

A simple model that represents the characteristic features of an artificial heart valve is a circular wire embedded in a homogeneous dielectric medium. In this section, three specific configurations containing such a circular wire are considered. First, we represent a completely broken heart valve by a perfectly conducting circular wire with an interruption. Second, we close the circular wire to obtain a simple model representing a perfect valve. Third, we include an impedance in the circular wire to model fatigue or a partial fracture. For each configuration, the relevant integral equation is formulated. Finally, we consider the dielectric properties of the surrounding medium.

### A. Open Loop

We consider a perfectly conducting thin wire, whose central axis is circular, with radius  $b$ , placed in the plane  $z = 0$  of a three-dimensional cylindrical coordinate system. The center of this circle coincides with the origin of a cylindrical coordinate system with  $\phi \in (-\pi, \pi]$ . The cross section of the wire is circular with radius  $a$ . The wire has an interruption for  $|\pi - \phi| < \phi_{\max}$  and is excited by a delta-gap source at  $\phi = \phi_{\text{gap}}$  or by an incident field generated by external sources. The configuration is illustrated in Fig. 3.

The electromagnetic behavior of the wire is completely determined by the integral equation for the total current in the angular direction. This equation can be obtained from the integral representation for the electric field due to a surface current in three

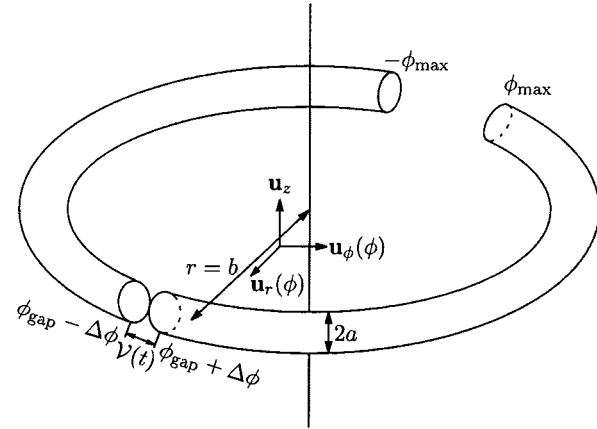


Fig. 3. Open circular loop and coordinate system.

dimensions, by considering  $E_\phi$  on the central axis of the wire. Since the surrounding medium is highly dispersive, it is convenient to formulate the equation in the time-Laplace domain. After a few straightforward approximations, we obtain

$$\begin{aligned} & \int_{-\phi_{\max}}^{\phi_{\max}} b d\phi' \left( \frac{1}{b^2} \partial_\phi^2 - \frac{s^2}{c^2} \cos(\phi - \phi') \right) \\ & \cdot \frac{\exp(-sR_a(\phi - \phi')/c)}{4\pi R_a(\phi - \phi')} I(\phi', s) \\ & = -\varepsilon s \left[ \frac{1}{b} V(s) \delta(\phi - \phi_{\text{gap}}) + E^i(\phi, s) \right]. \end{aligned} \quad (1)$$

In (1),  $s = \beta - i\omega$  is a complex frequency,  $I(\phi, s)$  denotes the total current along the wire,  $R_a(\phi) = \sqrt{4b^2 \sin^2(\phi/2) + a^2}$ ,  $\varepsilon$  and  $c$  are the permittivity and the complex wave velocity of the surrounding medium,  $V(s)$  is the voltage across the delta gap, and  $E^i(\phi, s)$  is the component of the incident electric field along the central axis. In analogy with the definitions for a straight wire [3], we refer to this equation as *Pocklington's equation*.

Numerically evaluating the differentiations with respect to  $\phi$  in (1) would strongly magnify the almost singular behavior of the kernel at  $\phi' = \phi$ . This may give rise to numerical problems. As an alternative, the operator is inverted in closed form. To this end, we use the one-dimensional Green's function that can be expressed as the solution of the inhomogeneous second-order differential equation

$$[\partial_\phi^2 - \gamma^2] G(\phi, \phi'; \gamma) = -\delta(\phi - \phi') \quad (2)$$

with  $\gamma = sb/c$ , which satisfies the radiation condition as  $|\phi| \rightarrow \infty$ . This solution is given by

$$G(\phi - \phi'; \gamma) = \frac{1}{2\gamma} \exp(-\gamma|\phi - \phi'|). \quad (3)$$

Extracting the behavior of the term  $\cos(\phi - \phi')$  for  $\phi' \approx \phi$  in (1)

and substituting the proper value of  $\gamma$  then results in

$$\begin{aligned}
 & \int_{-\phi_{\max}}^{\phi_{\max}} bd\phi' \frac{\exp[-sR_a(\phi-\phi')/c]}{4\pi R_a(\phi-\phi')} I(\phi', s) \\
 & - \frac{sb}{2c} \int_{-\phi_{\max}}^{\phi_{\max}} d\phi' \left\{ \exp[-sb|\phi-\phi'|/c] \right. \\
 & \quad \cdot \int_{-\phi_{\max}}^{\phi_{\max}} bd\phi'' [1-\cos(\phi'-\phi'')] \\
 & \quad \cdot \left. \frac{\exp[-sR_a(\phi'-\phi'')/c]}{4\pi R_a(\phi'-\phi'')} I(\phi'', s) \right\} \\
 & = \frac{Y}{2} \int_{-\phi_{\max}}^{\phi_{\max}} bd\phi' E^i(\phi', s) \exp[-sb|\phi-\phi'|/c] \\
 & + \frac{Y}{2} V(s) \exp[-sb|\phi-\phi_{\text{gap}}|/c] \\
 & + F_+(s) \exp[-sb(\phi+\phi_{\max})/c] \\
 & + F_-(s) \exp[-sb(\phi_{\max}-\phi)/c] \quad (4)
 \end{aligned}$$

where  $Y = \sqrt{\varepsilon/\mu}$  denotes the wave admittance of the medium surrounding the wire. The yet unknown signals  $F_+(s) \exp[-sb(\phi+\phi_{\max})/c]$  and  $F_-(s) \exp[-sb(\phi-\phi_{\max})/c]$  represent two independent homogeneous solutions of the differential equation (2). These signals can be determined by imposing the boundary conditions  $I(-\phi_{\max}, s) = I(\phi_{\max}, s) = 0$ . The subscripts “+” and “-” refer to the direction of propagation of the wave in the positive and negative  $\phi$ -directions, respectively. In analogy with the case of the single wire [3], (4) is referred to as *Hallén’s equation* for a circular wire with an interruption.

### B. Closed Loop

As a model of a perfect valve, we consider a completely closed circular wire. Pocklington’s equation (1) also holds for this configuration, with  $\phi_{\max} = \pi$ . In the derivation of Hallén’s equation, however, different boundary conditions must be applied. The most convenient procedure is to impose periodic boundary conditions on the Green’s function  $G$ . If we choose the angular domain as  $\phi \in [0, 2\pi)$ , the boundary conditions can be expressed as

$$G(\phi, \phi'; \gamma)|_{\phi=0} = G(\phi, \phi'; \gamma)|_{\phi=2\pi}$$

and

$$\partial_\phi G(\phi, \phi'; \gamma)|_{\phi=0} = \partial_\phi G(\phi, \phi'; \gamma)|_{\phi=2\pi}. \quad (5)$$

The solution of (2) that satisfies the boundary conditions (5) is given by

$$\begin{aligned}
 G(\phi, \phi'; \gamma) &= \frac{\cosh[(|\phi-\phi'| - \pi)\gamma]}{2\gamma \sinh(\pi\gamma)} \\
 &= \frac{1}{2\gamma} \sum_{n=-\infty}^{\infty} \exp[-\gamma|\phi-\phi' + 2\pi n|]. \quad (6)
 \end{aligned}$$

By comparing the second expression with (3), it is obvious that this is the  $2\pi$ -periodic solution of (2) with  $-\infty \leq \phi \leq \infty$ . This leads to the conclusion that imposing periodic boundary conditions on  $G$  is equivalent with a  $2\pi$ -periodic extension of the source over the infinite interval  $-\infty < \phi < \infty$ . To keep the expressions comparable to the case of the interrupted wire, we write  $G(\phi - \phi', \gamma) = \tilde{G}(\phi - \phi'; \gamma)/2\gamma$  where  $\tilde{G}$  is again a dimensionless quantity. Following a similar procedure as in Section II-A, we then arrive at Hallén’s equation for the closed circular loop

$$\begin{aligned}
 & \int_0^{2\pi} bd\phi' \frac{\exp[-sR_a(\phi-\phi')/c]}{4\pi R_a(\phi-\phi')} I(\phi', s) \\
 & - \frac{sb}{2c} \int_0^{2\pi} d\phi' \left\{ \tilde{G}\left(\phi-\phi', \frac{sb}{c}\right) \right. \\
 & \quad \cdot \int_0^{2\pi} b d\phi'' [1-\cos(\phi'-\phi'')] \\
 & \quad \cdot \left. \frac{\exp[-sR_a(\phi'-\phi'')/c]}{4\pi R_a(\phi'-\phi'')} I(\phi'', s) \right\} \\
 & = \frac{Y}{2} \int_0^{2\pi} b d\phi' \tilde{G}\left(\phi-\phi', \frac{sb}{c}\right) E^i(\phi', s) \\
 & + \frac{Y}{2} V(s) \tilde{G}\left(\phi-\phi_{\text{gap}}, \frac{sb}{c}\right) \quad (7)
 \end{aligned}$$

with  $\phi \in [0, 2\pi)$ .

### C. Partial Fracture

Finally, we create a simple model that can be used to represent a partial fracture or fatigue. Suppose that we place an impedance  $Z_{\text{load}}$  in the gap between the end faces of a broken wire at  $\phi = \phi_{\text{load}} - \Delta\phi$  and  $\phi = \phi_{\text{load}} + \Delta\phi$ . The electric field over the impedance may be considered as pointing in the  $\phi$ -direction. By taking the limit for  $\Delta\phi \rightarrow 0$ , we then obtain

$$E_\phi(b\mathbf{u}_r(\phi), s) = \frac{1}{b} Z_{\text{load}} I(\phi_{\text{load}}, s) \delta(\phi - \phi_{\text{load}}). \quad (8)$$

This term may be incorporated in the integral equations in the same way as the delta-gap voltage. In Hallén’s equation (7) for the closed wire, this amounts to adding the term

$$\frac{Y}{2} Z_{\text{load}} \tilde{G}\left(\phi - \phi_{\text{load}}, \frac{sb}{c}\right) I(\phi_{\text{load}}, s) \quad (9)$$

to the left-hand side.

### D. Surrounding Medium

In the actual situation, the surrounding medium is strongly inhomogeneous. However, its most important property is the dispersive behavior of the permittivity. To obtain a qualitative indication of the influence of that behavior, we assume that the curved wires specified in the previous sections are embedded in a homogeneous dielectric with the properties of blood. For the frequency-range of interest, the permittivity of blood for  $s = -i\omega$  can be represented by fitting a four-term Debye model [4], [5] to the permittivity data from [6]. The results are shown in Fig. 4, where the imaginary part  $\varepsilon_r''(\omega) = \sigma(\omega)/\omega\varepsilon_0$ . From this

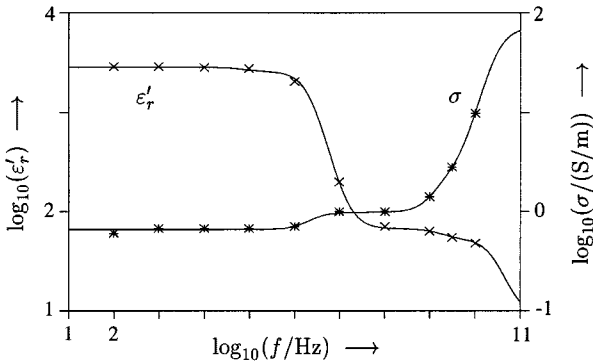


Fig. 4. Real part of the relative permittivity and conductivity as a function of frequency. Dots: experimental data. Solid lines: Debye model.

figure, we observe that we can realistically only hope to penetrate blood with an electromagnetic field up to  $f = \omega/2\pi = 500$  MHz.

### III. NUMERICAL SOLUTION AND RESULTS

The integral equations for the three model configurations can only be solved numerically. In this section, the method of solution is summarized and numerical results are presented.

#### A. Computational Approach

We first consider the solution of Hallén's equation (4) for the *open wire*. We normalize all space coordinates with respect to  $b$  and all time coordinates with respect to the corresponding free-space travel time, i.e.,  $\tilde{r} = r/b$  and  $\tilde{t} = c_0 t/b$ . Next, we discretize in space. The interval  $\phi \in (-\phi_{\max}, \phi_{\max})$  is divided into  $M$  equally spaced subintervals with mesh size  $\Delta\phi = 2\phi_{\max}/M$ . The points of observation are limited to  $\phi = \phi_m = -\phi_{\max} + m\Delta\phi$ , with  $m = 0, \dots, M$ . The integrals are now approximated. The almost singular behavior of the factor of  $1/4\pi R_a(\phi - \phi')$  for  $\phi' = \phi$  should be accounted for in the approximation. Therefore, we write

$$\begin{aligned} & \frac{\exp \left[ -s\sqrt{\epsilon_r} R_a(\phi_m - \phi') \right]}{4\pi R_a(\phi_m - \phi')} I(\phi', s) \\ & \approx \sum_{m'=1}^{M-1} \exp \left[ -s\sqrt{\epsilon_r} R_a(\phi_m - \phi_{m'}) \right] I(\phi_{m'}, s) \\ & \cdot \frac{\Lambda_{m'}(\phi')}{4\pi R_a(\phi_m - \phi')}, \end{aligned} \quad (10)$$

where  $\Lambda_m(\phi)$  is a triangular expansion function over the interval  $\phi \in [\phi_m - \Delta\phi, \phi_m + \Delta\phi]$ . The boundary conditions at the ends of the wire are automatically satisfied in this approximation. This restricts the integration to the closed-form evaluation of a set of weighting coefficients. The remaining integrals in (4) are approximated by a simple trapezoidal rule. The resulting discretized equation is second-order accurate as  $\Delta\phi \downarrow 0$  and has the same convolution symmetry as the continuous equation (4). This makes the discretized form extremely suitable for the application of the so-called conjugate-gradient fast Fourier transform (CGFFT) method [7], [8].

For the *loaded wire*, we essentially follow the same approach as described above. The main difference is that the current  $I(\phi, s)$  no longer vanishes at  $\phi = \pm\phi_{\max} = \pm\pi$ . Therefore, the summation over  $m'$  in (10) must be augmented by a term with  $m' = 0$ . Further, the sampled current  $I(\phi_m, s)$  and the discretized kernels are now periodic functions of  $m$  and  $m'$ . Therefore, there is no need to avoid aliasing effects in the evaluation of the convolution terms in the discretized integral equation and its adjoint. This means that these terms can now be evaluated with fast Fourier transform (FFT) operations of order  $M$ .

For the *closed wire*, we again use the same space discretization. The inversion is now even more simple. Subjecting the discretized equation to a discrete Fourier transformation directly leads to an expression for each of the Fourier coefficients of the discretized current in terms of the voltage and the Fourier coefficients of the incident field and the discretized kernel. An inverse FFT then directly produces the discretized current. Again, both transformations are of order  $M$ .

Finally, we want to display the results as a function of time. The necessary transformation is carried out via Bromwich inversion over  $s = \beta - i\omega$  with  $-\infty < \omega < \infty$ , where  $\beta \geq 0$ . We truncate the integral at some maximum frequency  $\omega = N\Delta\omega$ , and choose the time and frequency steps such that  $\Delta t\Delta\omega = 2\pi/N$ . A straightforward trapezoidal rule then reduces the integral over  $\omega$  into a sum that can be evaluated by an FFT of order  $N$ . The only possible complications are that, from a numerical point-of-view,  $\beta$  may not be too large, and that the Debye model mentioned in Section II-D must be generalized to complex frequencies by replacing  $\omega$  by  $is$ .

#### B. Results and Discussion

We first consider the situation where the circular wire is excited by an impressed delta-gap voltage. In Fig. 5, we look at two configurations that represent the extremes: namely, a perfect artificial heart valve and a completely fractured artificial heart valve. Further, we consider loads of 2.0, 8.0, and  $10^6 \Omega$ . The loads and gap are located at  $\phi = \pi$ . The dimensions are chosen such that they are representative of an actual artificial heart valve. The opening representing complete fracture is set at  $1^\circ$ , i.e.,  $\phi_{\text{opening}} = 2(\pi - \phi_{\max}) = \pi/180$ . The wire is excited with a Gaussian voltage pulse of the form  $\mathcal{F}(t) = \exp\{-[(t - t_0)/t_p]^2\}$ , with  $t_p = 0.5$  ns and  $t_0 = 4t_p$  at  $\phi = -\pi/4$ . In the computations, the wires were subdivided into  $M = 64$  segments.

By comparing the results in Fig. 5, it is observed that, as long as the reflections at the end faces of the open wire do not influence the currents, both signals are identical. However, a significant difference is observed at later times. Namely, the current along the closed wire contains a stationary component, which is not present along the open wire. It can be shown in closed form that the magnitude of this stationary component is independent of the permittivity of the surrounding medium [5]. For  $Z_{\text{load}} = 2.0 \Omega$  and  $Z_{\text{load}} = 8.0 \Omega$ , the current exhibits an exponentially decaying behavior at late times, with a decay rate that is indicative of the value of  $Z_{\text{load}}$ . Provided that a partial fracture can indeed be modeled by a resistive load, this means that the quality of the loop can be assessed from this late-time

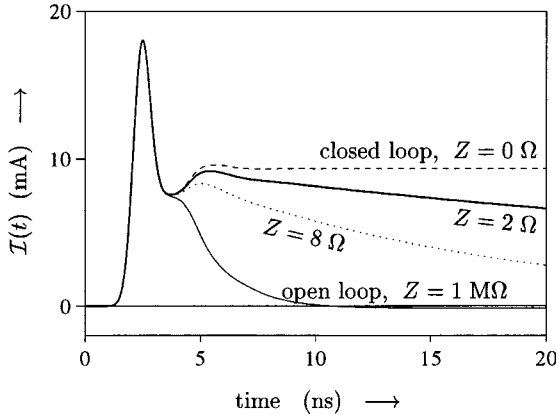


Fig. 5. Current along a closed, loaded, or open circular wire. Dimensions of the loop:  $a = 0.5$  mm,  $b = 2.0$  cm. Number of segments: 64, excitation point:  $\phi = -\pi/4$ , observation point:  $\phi = 0$ , position of load or opening:  $\phi = \pi$ .

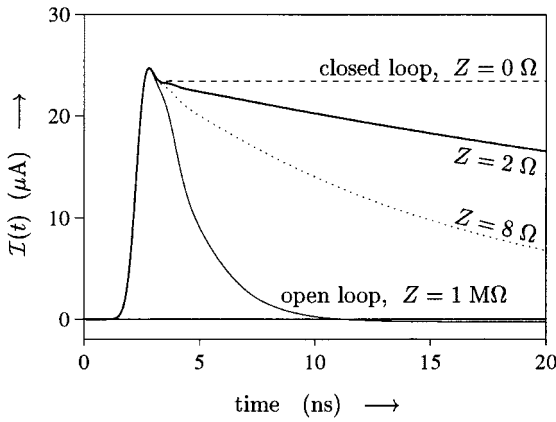


Fig. 6. Current along a circular wire, excited by a magnetic point dipole, located in the origin and pointing in the negative  $z$ -direction. Dimensions of the loop:  $a = 0.5$  mm,  $b = 2.0$  cm. Number of segments: 64, observation point:  $\phi = \pi/8$ .

behavior or, equivalently, from the low-frequency behavior of the generated current. Finally, the results for an open wire and for a wire loaded with an impedance of  $10^6 \Omega$  are graphically indistinguishable. This shows that we may also treat a broken wire as a closed wire with a large load.

Although a delta-gap voltage excitation can be approximated by a coil wound around a ferrite ring, the problem remains whether such a device can be positioned around the minor strut of an artificial heart valve. The same question arises for the detection of the current along the wire. A possible alternative is to remotely excite a current via a small antenna. In particular, we consider the current generated by a magnetic point dipole in an arbitrary point and pointing in an arbitrary direction. A magnetic current is a fictitious source, but the same effect can be generated by a small loop of electric current. The results for the same configuration as considered in Fig. 5 are shown in Fig. 6. Again, we observe a stationary current along the wire for the perfect loop. The introduction of an impedance causes an exponential decay in that current, with a decay rate that increases as the impedance increases.

#### IV. TWO COUPLED WIRES

Finally, we investigate whether it is possible to simultaneously excite and detect the current along the wire representing the artificial heart valve by using a second wire as a transmitting and receiving antenna. Such a wire could then be brought close to the valve via a catheter. In Section III-B, it was observed that a magnetic point dipole generates a current that strongly depends upon the status of the circular wire. Since the magnetic dipole is equivalent with a small current loop, it should be possible to generate similar effects with a second circular wire. The behavior of the current on the first wire, which represents the artificial heart valve, will then still depend on the status of that wire. This current, in turn, will induce a radiated field that will influence the current along the second wire. Based on the shape of the current along that “detection” wire, it should, therefore, be possible to determine the status of the wire “under test.”

##### A. Formulation of the Problem

We consider two perfectly conducting circular wires with radius  $b_1$  and  $b_2$ , placed in the planes  $z = 0$  and  $z = d$ , and centered around the  $z$ -axis. The cross sections are circular with radius  $a_1$  and  $a_2$ . The wires are embedded in a homogeneous, dielectric medium with permittivity  $\epsilon$ , permeability  $\mu$ , and wave velocity  $c = 1/\sqrt{\epsilon\mu}$ . Both wires can be excited by a delta-gap voltage and contain an impedance.

To derive the integral equation for the current on wire 1, we consider the electric field radiated by wire 2. When the distance between both wires is large compared to the thickness of wire 2, the current along that wire may be considered as being concentrated on the central axis. The integral representation for the  $\phi$ -component of the radiated field on the axis of wire 1 can then be written as

$$E_\phi^{\text{rad}}(b_1 \mathbf{u}_r(\phi), s) = \frac{1}{s\epsilon} \int_0^{2\pi} b_2 d\phi' \left[ \frac{1}{b_1 b_2} \partial_\phi^2 - \frac{s^2}{c^2} \cos(\phi - \phi') \right] \cdot \frac{\exp[-sR_{12}(\phi - \phi')/c]}{4\pi R_{12}(\phi - \phi')} I_2(\phi', s) \quad (11)$$

with

$$R_{12}(\phi) = \sqrt{b_1^2 + b_2^2 + d^2 - 2b_1 b_2 \cos(\phi)}. \quad (12)$$

The field given in (11) is now considered as an additional incident field in Pocklington's equation (1) for the current along wire 1. This changes (1) into

$$\begin{aligned} & \int_0^{2\pi} b_1 d\phi' \left[ \frac{1}{b_1^2} \partial_\phi^2 - \frac{s^2}{c^2} \cos(\phi - \phi') \right] \\ & \cdot \frac{\exp[-sR_1(\phi - \phi')/c]}{4\pi R_1(\phi - \phi')} I_1(\phi', s) \\ & + \int_0^{2\pi} b_2 d\phi' \left[ \frac{1}{b_1 b_2} \partial_\phi^2 - \frac{s^2}{c^2} \cos(\phi - \phi') \right] \\ & \cdot \frac{\exp[-sR_{12}(\phi - \phi')/c]}{4\pi R_{12}(\phi - \phi')} I_2(\phi', s) \\ & = \frac{\epsilon s}{b_1} Z_1 I_1(\phi_{\ell 1}, s) \delta(\phi - \phi_{\ell 1}) - \frac{\epsilon s}{b_1} V_1(s) \delta(\phi - \phi_{v1}) \end{aligned} \quad (13)$$

where  $R_1(\phi) = \sqrt{4b_1^2 \sin^2(\phi/2) + a_1^2}$ ,  $\phi_{\ell 1}$  is the position of the delta gap in which the impedance is located, and  $\phi_{v1}$  is the position of the delta gap across which the voltage is impressed. The extra subscript “1” indicates that these positions pertain to wire 1.

Analogously, we can substitute the radiated field from wire 1 into Pocklington’s equation wire for 2. This results in an integral equation that can also be obtained by interchanging the subscripts “1” and “2” in (13), and realizing that  $R_{21}(\phi) = R_{12}(\phi)$ . These two coupled integral equations determine the behavior of  $I_1$  and  $I_2$ .

### B. Results and Discussion

The coupled integral equations derived in Section IV-A are solved by the procedure explained for the single-wire models in Section III-A. Successively, equivalent Hallén-type equations are derived, dimensionless variables are introduced, the equations are discretized in space, and the discretized form is solved by the CGFFT method. Details can be found in [5].

In Fig. 7, we consider the situation where the second wire, i.e., the antenna, is excited by a delta-gap voltage. Since measurements of this type have to be invasive, the diameter of this ring is chosen smaller than the diameter of the ring representing the artificial heart valve. Both wires were subdivided into 64 equal segments. The second wire, which was driven by a Gaussian voltage pulse with parameters  $t_p = 0.5$  ns and  $t_0 = 4t_p$ , was placed 0.25 cm above the first one. Fig. 7 shows plots of the current along that second wire in case the first wire is loaded with 0, 2.0, 8.0, and  $10^6$   $\Omega$ , respectively. Since we are interested in the possibility of detecting a partial interruption on the basis of the shape of the current along the second wire, we only consider this current.

From Fig. 7, it is observed that the magnitude of the stationary component in the current along the wire representing the antenna is influenced by the status of the wire representing the heart valve. When the “valve” is intact, the stationary current component on the “antenna” is larger than for a completely broken “valve.” Introducing an impedance results in an exponential decay superimposed on a constant current. This effect is observed more clearly when one of the configurations is used as a reference. As an illustration, Fig. 7(b) shows the differences with the case where  $Z_1 = 10^6$   $\Omega$ .

### V. CONCLUSIONS

In this paper, we have studied the possibility of detecting mechanical defects in certain artificial heart valves by investigating a simple model configuration via computational simulations. The model consists of a circular thin-wire segment embedded in a homogeneous dispersive dielectric medium. To represent the characteristic features of an artificial heart valve, three specific configurations were considered, representing a perfect valve, a completely fractured valve, and fatigue or a partial fracture. In all three cases, the mathematical formulation proceeded in the same way. We started from a one-dimensional Pocklington-type integral equation for the current along the wire. To avoid numerical problems, we used a one-dimensional Green’s function

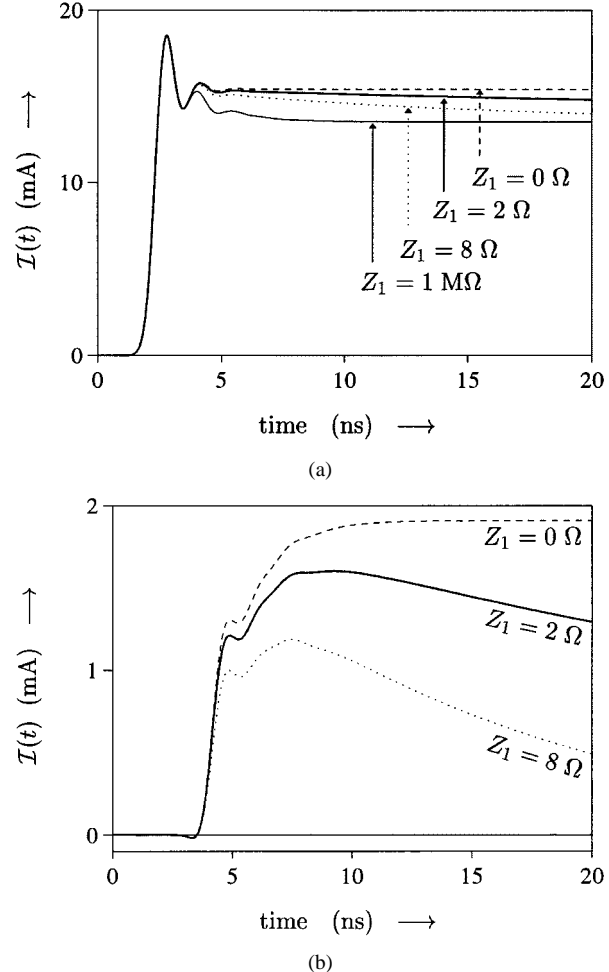


Fig. 7. Current along wire 2. Dimensions of the loops:  $a_1 = a_2 = 0.5$  mm,  $b_1 = 2.0$  cm,  $b_2 = 1.5$  cm. Distance between the wires: 2.5 mm. Number of segments: 64, excitation point (wire 2):  $\phi = 0$ , observation point (wire 2):  $\phi = \pi/2$ , position of load (wire 1):  $\phi = \pi$ . (a) No reference used. (b) Reference  $Z_1 = 10^6$   $\Omega$ .

technique to obtain an equivalent Hallén form. Since these integral equations could not be solved analytically, the unknown currents were determined numerically.

For the excitation, two possibilities were considered. First, we investigated a delta-gap voltage excitation. A significant difference was observed in the late-time behavior of the currents in the three configurations. On the basis of these characteristic differences, it seems possible to distinguish a perfect heart valve from a broken one. Since a delta-gap voltage may not be realizable from a physical point-of-view, we subsequently considered the case where the circular wire was excited by a more realistic source like a magnetic point dipole. The same significant effect in the late-time behavior of the current along the wire was noticed, as in the case of a delta-gap excitation. This means that, with this source, a current can be generated along the wire with a late-time behavior that depends strongly on the status of the wire.

Finally, the problem of detecting this difference in late-time behavior was addressed. A magnetic point dipole can also be envisaged as a small loop in which a current is switched on. Such a current can also be generated by exciting this small loop with a delta-gap voltage pulse. Therefore, a logical next step was

to replace the magnetic dipole by a secondary loop excited by a voltage source. Our expectation that such a loop may then serve as a transmitting, as well as a receiving, antenna was confirmed by the results.

It should be remarked that, until now, we have considered a relatively simple model of the actual configuration. If this study is continued, a mandatory next step is to include interior loops into the circular wire to obtain a more realistic model of the occluder struts. Also, the occluder itself may have to be taken into account. A second possible step is to take into account the wires connecting the secondary loop to the source and the impedance of such a source. Third, the fact that the artificial heart valve is located in a blood vessel could be taken into account by considering an inhomogeneous embedding.

Finally, because of the large number of assumptions in the present model, we preferred to obtain more experimental validation of our idea before a further generalization of the model was considered. While this validation was in progress, a noninvasive technique was discovered that may provide an indication of the presence of fractures. This has reduced the urgency of developing an invasive technique based on the electromagnetic detection. Nevertheless, both the problem and ideas resulting from our feasibility study seemed to be interesting enough to be reported to the scientific community.

#### ACKNOWLEDGMENT

The authors would like to thank Prof. B. A. J. M. de Mol, Department of Cardiopulmonary Surgery, Academic Medical Center, Amsterdam, The Netherlands, for bringing this subject to their attention. Further, the authors are indebted to Dr. A. P. J. van Deursen, Eindhoven University of Technology, Eindhoven, The Netherlands, for many stimulating discussions on the practical implementation of their ideas.

#### REFERENCES

- [1] Y. Van der Graaf, F. de Waard, L. A. van Herwerden, and J. J. Defauw, "Risk of strut fracture of Björk-Shiley valves," *Lancet*, vol. 339, pp. 257-261, 1992.
- [2] B. A. De Mol, M. Kallewaard, R. B. McLellan, L. A. van Herwerden, J. J. Defauw, and Y. van der Graaf, "Single-leg strut fractures in explanted Björk-Shiley valves," *Lancet*, vol. 343, pp. 9-12, 1994.
- [3] A. G. Tijhuis, Z. Q. Peng, and A. R. Bretones, "Transient excitation of a straight thin-wire segment: A new look at an old problem," *IEEE Trans. Antennas Propagat.*, vol. 40, pp. 1132-1146, Oct. 1992.
- [4] E. S. A. M. Lepelaars, "Electromagnetic pulse distortion in living tissue," *Med. Biol. Eng. Comput.*, vol. 34, pp. 213-220, 1996.
- [5] ———, "Transient electromagnetic excitation of biological media by circular loop antennas," Ph.D. dissertation, Faculty Elect. Eng., Eindhoven Univ. Technol., Eindhoven, The Netherlands, 1997.
- [6] K. R. Foster and H. P. Schwan, "Dielectric properties of tissues," in *CRC Handbook of Biological Effects of Electromagnetic Fields*, C. Polk and E. Postow, Eds. Boca Raton, FL: CRC Press, 1986, pp. 27-96.
- [7] T. K. Sarkar, "The application of the conjugate gradient method for the solution of operator equations arising in electromagnetic scattering from wire antennas," *Radio Sci.*, vol. 19, pp. 1156-1172, 1984.
- [8] P. M. Van den Berg, "Iterative schemes based on the minimization of the error in field problems," *Electromag.*, vol. 5, pp. 237-262, 1985.



**Eugène S. A. M. Lepelaars** (M'98) received the M.Sc. degree in applied mathematics and the Ph.D. degree from the Eindhoven University of Technology, Eindhoven, The Netherlands, in 1992 and 1997, respectively. His doctoral research was focused on electromagnetic excitation of biological media by a circular loop antenna.

In 1997, he was a Post-Doctoral Researcher at the University of Delaware, Newark, where he was involved with multicriteria optimization of antenna arrays. Since April, 1998, he has been with the Electromagnetic Effects Section, TNO Physics and Electronics Laboratory, The Hague, The Netherlands, where his principal research subject is computational electromagnetics.



**Willem D. R. van Ooijen** was born in Zwijndrecht, The Netherlands, in 1968. He received the B.Sc. degree in electrical engineering from the Polytechnic School of Rotterdam, The Netherlands, in 1993, and the M.Sc. degree in electrical engineering from the Eindhoven University of Technology, Eindhoven, The Netherlands, in 1996, respectively.

From 1996 to 1998, he was a Scientist with the Radar Group, TNO Physics and Electronics Laboratory, The Hague, The Netherlands. Since June 1998, he has been a Telecommunications Consultant with Arithmos Management Consultants B.V., The Hague, The Netherlands. His research interests are the analytical and numerical aspects of the theory of electromagnetic waves and antenna design.



**Anton G. Tijhuis** (M'88) was born in Oosterhout N.B., The Netherlands, in 1952. He received the M.Sc. degree in theoretical physics from Utrecht University, Utrecht, The Netherlands, in 1976 and the Ph.D. degree (*cum laude*) from the Delft University of Technology, Delft, The Netherlands, in 1987.

From 1976 to 1986 and 1986 to 1993, he was an Assistant and Associate Professor, Faculty of Electrical Engineering, in the Laboratory of Electromagnetic Research, Delft University of Technology. In 1993, he became a Full Professor of electromagnetics, Faculty of Electrical Engineering, at the Eindhoven University of Technology, Eindhoven, The Netherlands. He has been a Visiting Scientist at the Universities of Boulder (Boulder, CO), Granada (Spain), and Tel Aviv (Israel). His research interests are the analytical, numerical, and physical aspects of the theory of electromagnetic waves. In particular, he has been involved with the efficient techniques for the computational modeling of electromagnetic fields and their application to detection and synthesis problems from several areas of electrical engineering.